



The use of rice and coffee husks for biosorption of U (total), ^{241}Am , and ^{137}Cs in radioactive liquid organic waste

Rafael Vicente de Pádua Ferreira¹ · Leandro Goulart de Araujo² · Rafael Luan Sehn Canevesi³ · Edson Antonio da Silva³ · Eduardo Gurzoni Alvares Ferreira² · Maurício Cesar Palmieri¹ · Júlio Takehiro Marumo²

Received: 26 February 2020 / Accepted: 12 June 2020 / Published online: 20 June 2020
© Springer-Verlag GmbH Germany, part of Springer Nature 2020

Abstract

Rice and coffee husks (raw and chemically activated) are examined as potential biosorption materials regarding their capacity to remove U (total), ^{241}Am , and ^{137}Cs . The physical parameters evaluated were the morphological characteristics of the biomass, real and apparent density, and surface area. Contact times for the batch experiments were 0.5, 1, 2, and 4 h, and the concentrations tested ranged between 10% of the total concentration and the radioactive waste itself without any dilution. The results were evaluated by experimental sorption capacity, ternary isotherm, and kinetics models. The kinetics results showed that equilibrium was reached after 2 h for all biomass. Raw coffee husk showed the best adsorption results in terms of maximum capacity (q_{max}) for all three radionuclides, which were 1.96, 39.4×10^{-6} , and 46.6×10^{-9} mg g⁻¹ for U, Am, and Cs, respectively. The biosorption process for the raw and activated rice husks was best represented by the Langmuir ternary isotherm model with two sites. For the coffee husk, in the raw and activated states, the biosorption process was best described by the modified Jain and Snoeyink ternary model. These results suggest that biosorption with these biomaterials can be applied in the treatment of liquid organic radioactive waste containing mainly uranium and americium.

Keywords Biosorption · Coffee husk · Rice husk · Uranium · Americium · Caesium

Introduction

In the field of biosorption, most studies have been conducted with sorption of heavy metals and related elements, including actinides, lanthanides, and metalloids. Among biosorbents, agricultural residues stand out, being low-cost materials with

sustainable use. The literature describes the efficiency of agricultural residues in biosorption (Liao et al. 2004; Kumar and Bandyopadhyay 2006; Krishnani et al. 2008; Li et al. 2010), including rice husk and rice straw (Mishra et al. 2007; Rocha et al. 2009), and coffee husk (Oliveira et al. 2008a; Alhogbi 2017).

Rice husk is insoluble in water; has good chemical stability; has high mechanical strength; and has functional groups in its structure such as OH, Si-OH, C-H, C=O, C=C, CH₂, CH₃, CO, Si-O-Si, C-C, Si-H, and -O-CH₃, which confer qualities as an adsorbent material for heavy metal treatment in aqueous effluent (Mishra et al. 2007; Ma et al. 2011). Coffee husk also has interesting functional groups in relation to its adsorbent capability, such as -OH, -COOH, and C=O. The biosorption capacity of these materials may be improved by modifying their structure with chemical treatments, which may increase the active bond sites, improve the ion exchange properties, and generate new functional groups, promoting better metal absorption (Mishra et al. 2007; Wan Ngah and Hanafiah 2008; Rocha et al. 2009). Biosorption can be thus a feasible, cheap, effective, and easy method for the treatment of liquid organic radioactive waste (LORW).

Responsible editor: Tito Roberto Cadaval Jr

Electronic supplementary material The online version of this article (<https://doi.org/10.1007/s11356-020-09727-8>) contains supplementary material, which is available to authorized users.

✉ Leandro Goulart de Araujo
lgoulart@alumni.usp.br

¹ Itatijuca Biotech, Av. Prof. Lineu Prestes, São Paulo 05508-000, Brazil

² Serviço de Gerência de Rejeitos Radioativos, Instituto de Pesquisas Energéticas e Nucleares, Av. Prof. Lineu Prestes, São Paulo 05508-000, Brazil

³ Centro de Engenharias e Ciências Exatas, 645 Rua da Faculdade, Toledo, PR 85903000, Brazil

There is a considerable amount of literature on biosorption of uranium, including by bacteria (Wei et al. 2019; Wang et al. 2019), yeast (Bai et al. 2010; Lu et al. 2013; Zheng et al. 2018), algae (Bağda et al. 2017), macrophytes (Yi et al. 2016a; Vieira et al. 2019), pollen pini (Wang et al. 2015), black hair (Saini and Melo 2015), and fungi (Wang et al. 2010; Pang et al. 2011). Biosorption of americium is also found in the literature, using biomaterials including fungi (Dhami et al. 2002; Luo et al. 2003; Liao et al. 2004) and yeast (Liu et al. 2002). Biosorption of caesium is scarce in the literature. Examples of biosorbents are mucilaginous seeds (Chakraborty et al. 2007), rice husk (Mishra et al. 2007), and microalgae (Lee et al. 2019).

Nevertheless, most researchers have used a simple adsorption isotherm models to explain the adsorption behaviour in the presence of multi-metals in solutions. For the accurate design of the biosorption separation processes, the adsorption equilibrium and kinetics are addressed in this work. While the equilibrium data provide the efficacy of biosorption, the kinetics experiments give the optimal conditions for a full-scale process (Febrianto et al. 2009).

Rice and coffee husks were chosen as biosorbents in this work, because these materials have presented interesting results for the removal of non-desirable compounds or metals. For instance, Raoul et al. (2014) showed that rice and coffee husks are suitable for adsorbing phenol from aqueous solution. Ajmal et al. (2003) indicated that rice husk can be utilised as an adsorbent for the removal of Cd(II) from wastewater. Oliveira et al. (2008a) used coffee husks effectively as potential biosorbents for the treatment of dye-contaminated waters and (Oliveira et al. 2008b) in the removal of heavy metals from aqueous solutions.

In this work, the capacity of rice and coffee husks was evaluated, before and after chemical treatment, for removing U (total), ^{241}Am , and ^{137}Cs from LORW. As far as we know, these biomaterials have not been previously addressed for their capacity to remove multicomponent radionuclides from this type of waste. Moreover, detailed kinetics models have not been previously discussed for the biosorption process with rice and coffee husks as biosorbents. In the present work, ternary kinetics models are therefore proposed for this process, considering the radionuclides U (total), ^{241}Am , and ^{137}Cs . The results obtained in this study can be applied directly to the scaling up and process design, since the kinetics constants obtained take into consideration all species present in the LORW.

Materials and methods

Assessment of the ability of rice and coffee husks to remove U (total), ^{241}Am , and ^{137}Cs in waste was performed using rice and coffee husks in raw and activated forms. The radioactive

liquid studied was composed of water; ethyl acetate (196 mg L^{-1}); tributyl phosphate (227 mg L^{-1}); and the radionuclides U (total), ^{241}Am , and ^{137}Cs . The pH value was 2.17, since there is a significant amount of nitric acid in the liquid waste. The concentrations of the radionuclides in this real radioactive waste were U (total) = $(1.100 \pm 0.086) \times 10^2\text{ mg L}^{-1}$, $^{241}\text{Am} = (1.800 \pm 0.002) \times 10^{-3}\text{ mg L}^{-1}$, and $^{137}\text{Cs} = (6.800 \pm 0.001) \times 10^{-6}\text{ mg L}^{-1}$. This waste was generated from research and development activities in the nuclear fuel reprocessing field. More information on the characteristics of this waste is provided elsewhere (Ferreira et al. 2012).

This work was divided into three stages: i) preparation and activation of the rice and coffee husks, ii) physical characterisation of the biomass, and iii) batch biosorption experiments. The biosorption process was analysed by ternary isotherm and kinetics models.

Preparation of biomass

The rice and coffee husks were produced by Arroz Vale do Sul® and Grupo Sara Lee®, respectively. The husks were washed with distilled water, oven-dried (Fanem, Brazil) at $80\text{ }^\circ\text{C}$ for 24 h, sterilised by UV radiation (Hexiclean, China), chopped, and sieved (Telastem, Brazil) to obtain particle sizes between 0.297 and 0.500 mm. Part of the biomass was used directly in batch biosorption experiments (so-called raw husk), and part was separated to carry out an activation procedure through chemical modification (so-called activated husk).

Activation of biomass

The husks were activated by chemical modification according to the procedure described by Rocha et al. (2009). Activation was performed with the addition of 1.0 mol L^{-1} of HNO_3 solution (Merck, Brazil) and 0.75 mol L^{-1} of NaOH (Merck, Brazil) to 10 g of triturated biomass, followed by filtration (slow filtration, $\text{Ø} = 0.45\text{ }\mu\text{m}$) (Millipore, USA) and washing steps, and subsequent heating at $60\text{ }^\circ\text{C}$ (Ferreira et al. 2018).

Physical characterisation

The physical properties (both raw and activated) of the rice and coffee husks were also analysed. Morphological characteristics of the husks were evaluated by scanning electron microscopy (Model XL30, Philips, Netherlands). The real density was determined by helium pycnometry (Model 1330, Micromeritics, USA), and the apparent density was determined by weight/volume comparison. Finally, the surface area of the biosorbents was determined by using the BET method (ASAP 2010 apparatus, Micromeritics, USA), based on nitrogen adsorption–desorption isotherms at 77 K.

Biosorption experiments

Biosorption experiments were performed using 0.2 g of rice or coffee husk suspended in 10 mL of solutions prepared with distillate water and the LORW diluted to a concentration range of radionuclides from 10 to 100%. The suspensions were shaken (150 rpm) at room temperature for 2 h. At the end of the experiment, the biomass was separated by filtration. The concentration of each radioisotope remaining in the filtrate was determined by inductively coupled plasma optical emission spectrometry (ICP-OES) and gamma spectrometry. All experiments were performed in triplicate. All results are given by their mean ± standard deviation.

Determination of U (total) by ICP-OES

The total uranium in the samples was quantified by ICP-OES (model 7000DV, PerkinElmer, USA). To perform the analysis, a calibration curve was prepared using a standard uranium solution (Matthey Johnson Company). The wavelength (λ) used in the determination of the uranium was 385.466 nm, and the result is expressed as the average of triplicate measurements.

Determination of ²⁴¹Am and ¹³⁷Cs by gamma spectrometry

¹³⁷Cs and ²⁴¹Am measurements were carried out by gamma spectrometry (Canberra Industries, USA, model GX4510 HPGe detector with a beryllium window of 0.5-mm thickness). The detector shielding is composed of a lead wall (thickness 105 mm), copper wall (2 mm), and lucite wall (4 mm). ¹³⁷Cs and ²⁴¹Am activity concentrations were calculated by using the following specific energy photopeaks: 661.66 and 59.54 keV, respectively.

Fourier transform infrared analysis

The functional groups present in the biomass were analysed with an absorption spectrometer in the Fourier transform infrared analysis (FTIR) region (Bomem MB brand, arid-zone series, Model-MB104, Canada). For this analysis, pellets containing 5 mg of biomass and 200 mg of KBr were prepared, and infrared spectra were obtained in the region of 400–4000 cm⁻¹.

Mathematical modelling of the biosorption process

Equation 1 describes the metal uptake of species *j* by the biosorbent:

$$q_j = \frac{(C_{ij} - C_{jf})V}{m_{\text{bio}}} \quad \begin{matrix} j = \text{Total U, } ^{241}\text{Am, or } ^{137}\text{Cs} \\ \text{bio} = \text{rice or coffee husk} \end{matrix} \quad (1)$$

where *C_{ij}* and *C_{jf}* are the initial and final concentration of metal species *j* in solution (mg L⁻¹), *m_{bio}* is the dry mass of biosorbent (0.2 g), and *V* is the volume of solution (1 × 10⁻² L).

Equilibria and capacity relationships for monocomponent systems are well known as well as their numerous types of adsorption isotherm. Modelling adsorption in multicomponent systems is known to be more complex than that in a monocomponent system, since there are more effects to be included in those models. As mentioned earlier, this complexity is due to the types of response when two or more metal ions are involved in the biosorption process: synergism, antagonism, and non-interaction (Ting et al. 1991).

Studies on the use of biosorption are scarce in the treatment of real liquid radioactive waste. For this reason, the modelling of multicomponent adsorption in LORW is little known. In a previous work, Ferreira et al. (2018) employed coconut fibre to treat radioactive waste. The authors evaluated ternary kinetics and isotherm models, which were effective for estimating the simultaneous biosorption of uranium, americium, and caesium in LORW. The need for improvement has led them to new biosorption tests with different biosorbents.

In this report, we examine models based on Langmuir, and Jain and Snoeyink models for ternary systems to evaluate the biosorption of U (total), ²⁴¹Am, and ¹³⁷Cs in the biomass. The four models used to describe the biosorption equilibrium were the Langmuir ternary adsorption model, Langmuir ternary with two sites, the Jain and Snoeyink ternary model; and the modified Jain and Snoeyink ternary model (Table 1).

These models were selected based on the results obtained through FTIR, from which several functional groups that can act as sites in the adsorption process were identified. Therefore, the hypothesis of considering two types of site with different energies is justified.

Also, two kinetics models were used to describe the biosorption of U (total), ²⁴¹Am, and ¹³⁷Cs in the biomass. From the equilibrium model that best represented the equilibrium data, the selected model was used to represent the biosorption kinetics for each biosorbent material.

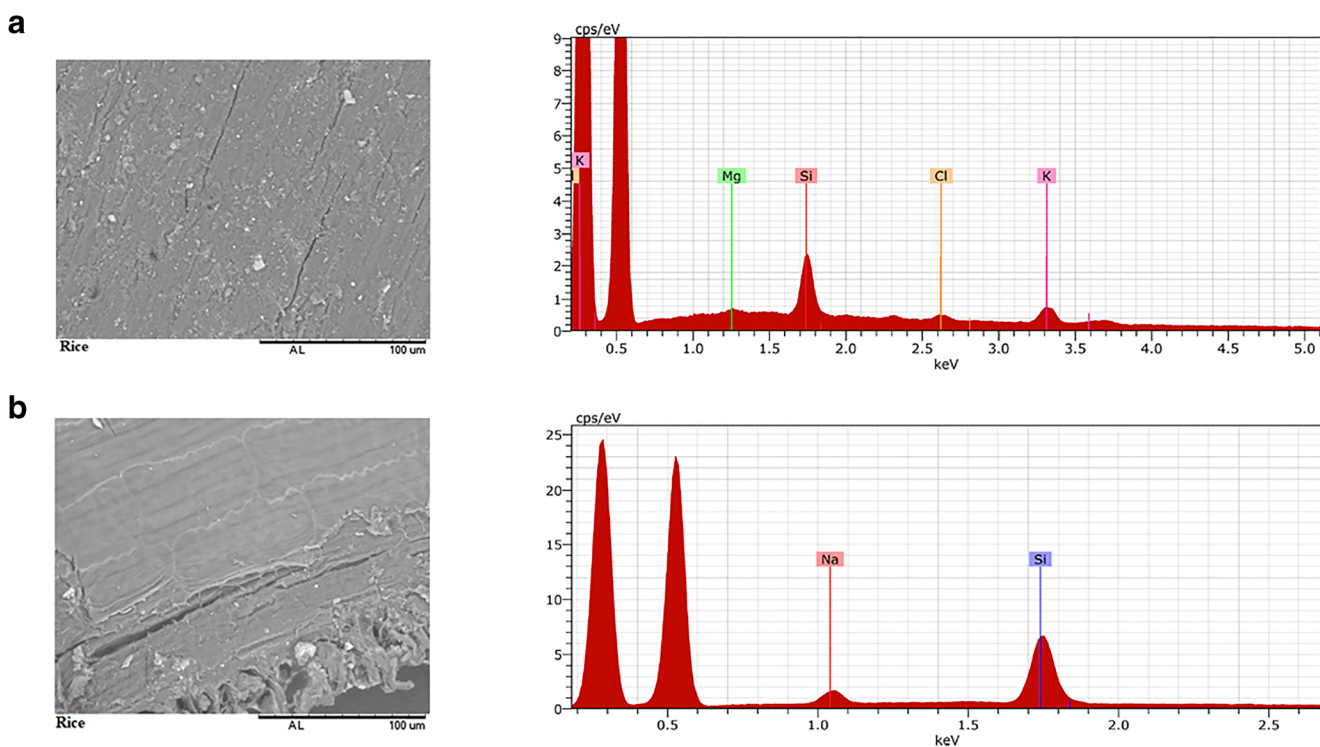
As the ion concentrations differ by orders of magnitude, depending on the radionuclide, all data were normalised. This procedure ensures better parameter adjustment for all adjusted variables regardless of the order of magnitude. The parameters of the model isotherms were estimated by using a nonlinear least-squares objective function minimised with the Nelder-Mead simplex algorithm (in *Maple*), which gives Eq. 12:

$$F = \sum_{j=1}^n (q_U^{\text{EXP}} - q_U^{\text{MOD}})^2 + (q_{\text{Am-241}}^{\text{EXP}} - q_{\text{Am-241}}^{\text{MOD}})^2 + (q_{\text{Cs-137}}^{\text{EXP}} - q_{\text{Cs-137}}^{\text{MOD}})^2 \quad (12)$$

where *F* is the objective function; *n* is the number of experimental data; *q_U^{EXP}*, *q_{Am-241}^{EXP}*, and *q_{Cs-137}^{EXP}* represent,

Table 1 Adsorption isotherm models used to describe data. Adapted from Ferreira et al. (2018)

Model, number of parameters, and description	Equation	No.
• Langmuir ternary adsorption	$q_1 = \frac{q_{mC}C_1b_1}{1+b_1C_1+b_2C_2+b_3C_3}$	(2)
• Four parameters	$q_2 = \frac{q_{mC}C_2b_2}{1+b_1C_1+b_2C_2+b_3C_3}$	(3)
• Considers competition for the three metals in the adsorption site occupation	$q_3 = \frac{q_{mC}C_3b_3}{1+b_1C_1+b_2C_2+b_3C_3}$	(4)
• Langmuir ternary with two sites	$q_1 = \frac{q_{mU}C_1b_{U1}}{1+b_1C_1}$	(5)
• Five parameters	$q_2 = \frac{q_{mC}C_2b_2}{1+b_2C_2+b_3C_3}$	(6)
• Considers that metal 1 occupies only a fraction of sites q_{mU} (without competition). In the other fraction of sites (q_{mC}), there is a (binary) competition for metals 2 and 3	$q_3 = \frac{q_{mC}C_3b_3}{1+b_2C_2+b_3C_3}$	(7)
• Ternary Jain and Snoeyink	$q_1 = \frac{q_{mU}C_1b_1}{1+b_1C_1} + \frac{q_{mC}C_1b_1}{1+b_1C_1+b_2C_2+b_3C_3}$	(8)
• Five parameters	$q_2 = \frac{q_{mC}C_2b_2}{1+b_1C_1+b_2C_2+b_3C_3}$	(9)
• Considers that metal 1 occupies only a fraction of sites q_{mU} (without competition). In the other fraction of sites (q_{mC}), there is a (ternary) competition for metals 1, 2, and 3; in addition, the interaction forces between the two types of site (q_{mU} and q_{mC}) for species 1 are the same	$q_3 = \frac{q_{mC}C_3b_3}{1+b_1C_1+b_2C_2+b_3C_3}$	(10)
• Modified Jain and Snoeyink ternary	$q_1 = \frac{q_{mU}C_1b_{U1}}{1+b_1C_1} + \frac{q_{mC}C_1b_1}{1+b_1C_1+b_2C_2+b_3C_3}$	(11)
• Six parameters	$q_2: \text{ same as Eq. 9}$	
• Considers that metal 1 occupies only a fraction of the sites q_{mU} (without competition). In the other fraction of the sites (q_{mC}), there is a (ternary) competition for metals 1, 2, and 3; in addition, the interaction forces between the two types of site (q_{mU} and q_{mC}) for species 1 are different	$q_3: \text{ same as Eq. 10}$	

**Fig. 1** SEM image (left) and corresponding EDS spectra (right) of **a** raw rice husk and **b** activated rice husk. Mass percentages (norm.). **a** Si (50.00%), K (40.52%), Cl (7.62%), and Mg (1.86%). **b** Si (90.10%) and Na (9.90%)

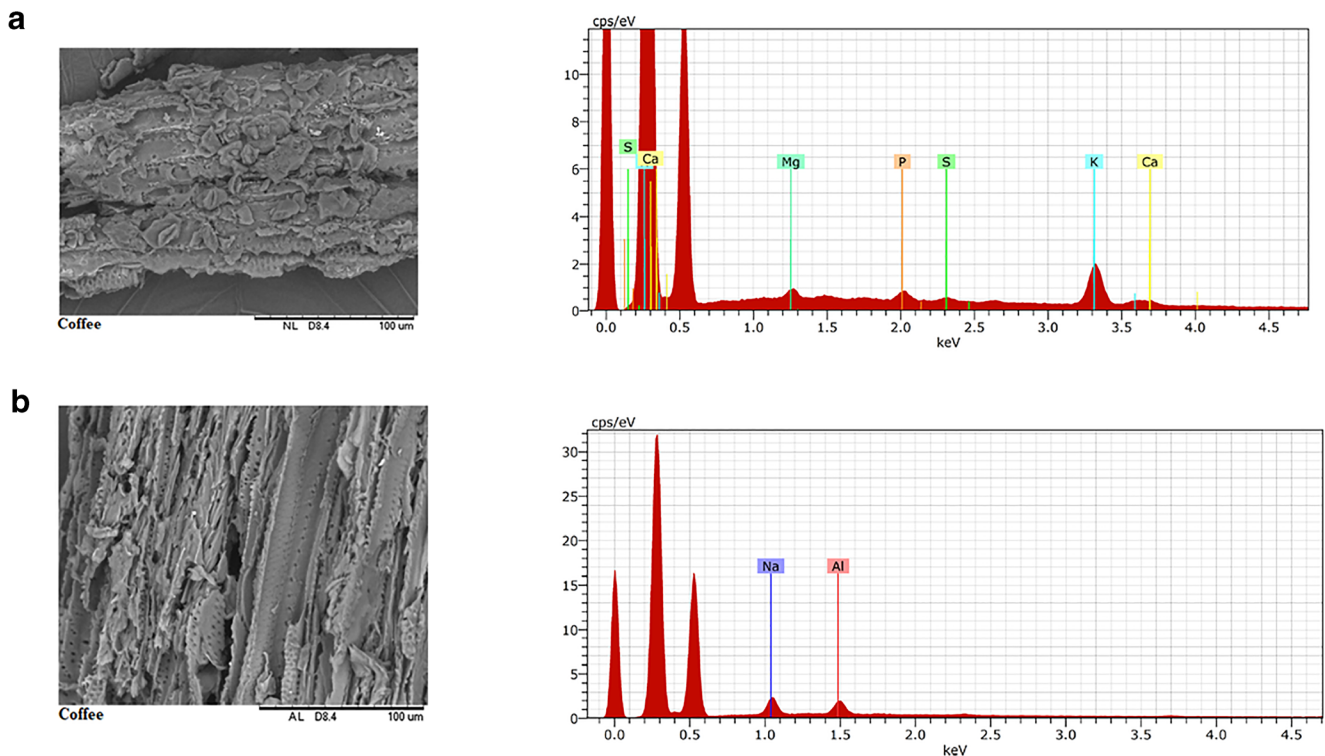


Fig. 2 SEM image (left) and corresponding EDS spectra (right) of **a** coffee raw husk and **b** activated coffee husk. Mass percentages (norm.). **a** K (64.11%), Mg (11.81%), Ca (11.75%), P (8.27%), and S (4.06%). **b** Al (58.37%) and Na (41.63%)

respectively, the experimental concentrations of ions in the biosorbent species U (total), ^{241}Am , and ^{137}Cs ; and $q_{\text{U}}^{\text{MOD}}$, $q_{\text{Am-241}}^{\text{MOD}}$, and $q_{\text{Cs-137}}^{\text{MOD}}$ represent, respectively, the concentrations of ions species U (total), ^{241}Am , and ^{137}Cs in the biosorbent calculated by using the model.

Results and discussion

Physical characterisation

Figures 1 and 2 present the micrograph images of rice and coffee husks, respectively, before and after activation by scanning electron microscopy with energy-dispersive X-ray spectroscopy (SEM-EDS).

Modifications were observed on the surface of the activated forms caused by the acid/base (HNO_3/NaOH) solutions and by increased pore exposure. EDS spectra of the rice husk (Fig. 1) show the existence of three main peaks in its raw form (Fig. 1a): Si, K, and Cl. In contrast, the activated form indicated a predominant peak for Si (Fig. 1b). It is noteworthy that the rice husk may contain a significant amount of SiO_2 —14.8% of the total mass (Korotkova et al. 2016). EDS spectra of the raw coffee husk (Fig. 2a) show that this material has K, and lower amounts of Mg, Ca, P, and S. After activation (Fig. 2b), none of these compounds were observed. The presence of Na and

Al in the activated coffee husk is due to the activation process (Fig. 2b).

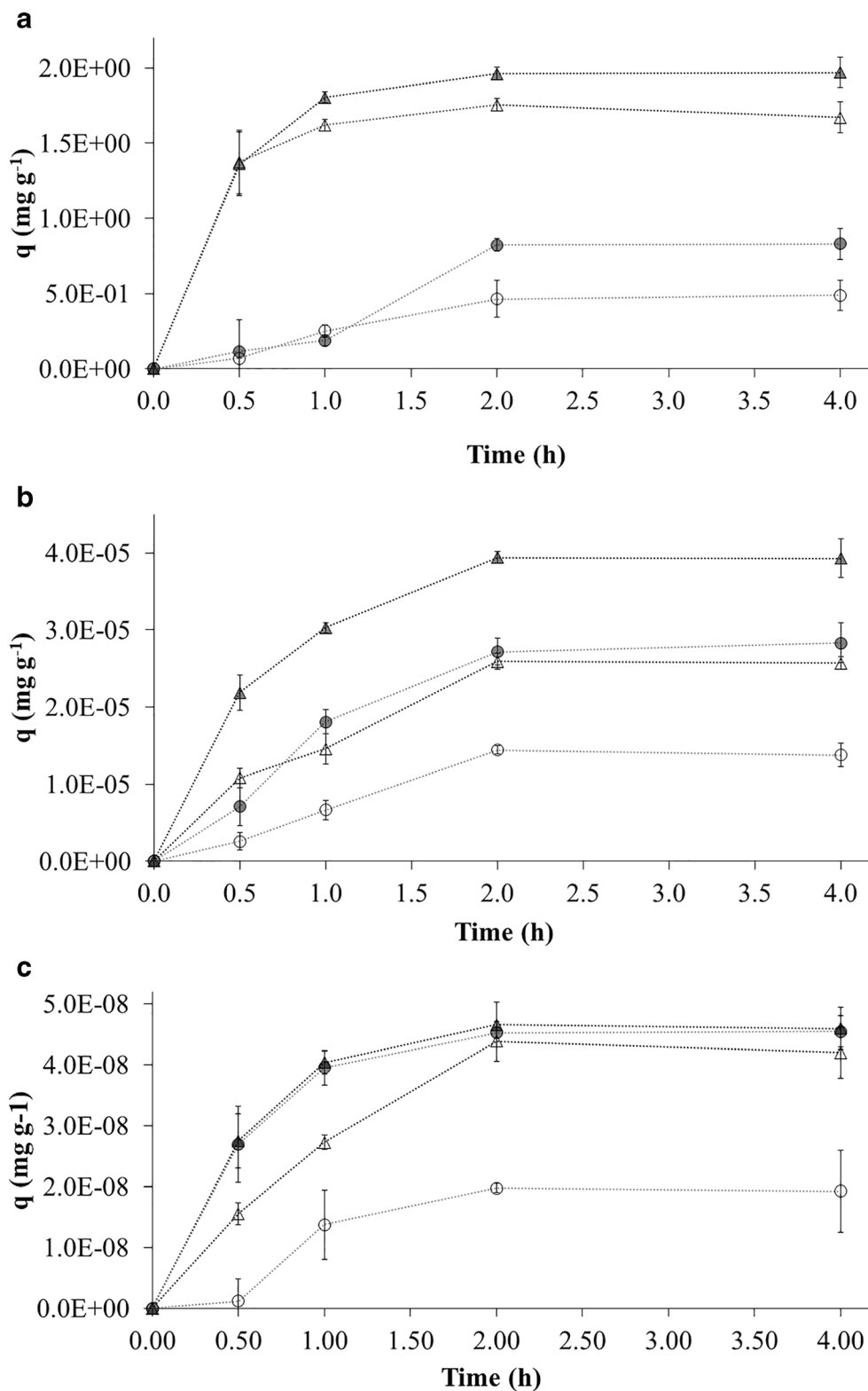
Real density, apparent density, and surface area

Table S1 details real and apparent densities, and the surface area of raw and activated husks. The real density is the specific weight of the solid phase of the particles or the density of the

Table 2 Functional groups of rice and coffee raw husks identified by FTIR

Biomass	Wavenumber (cm^{-1})	Functional groups
Rice husk	3451	–OH
	2882	–CH
	1733	–C=O
	1467	–CH ₂ and –CH ₃
	1066	–Si–O–Si, C–S–H, and –OH
Coffee husk	550	Si–H
	3430	–OH
	2925	–CH
	1654	–C=C
	1454	–COO [–]
	1029	–C–O–C
	816	–C–C

Fig. 3 Evolution of total uranium (a), americium (b), and caesium (c) biosorption as a function of time. \blacktriangle Raw coffee husk, \triangle Activated coffee husk, \bullet Raw rice husk, \circ Activated rice husk



particles themselves. The apparent density is the weight of the husks per unit volume and consists of the solid particles and the volume of their pores. The values of all parameters slightly decreased in the activated forms of the husks, which can be justified by the removal of material from the biomass surface.

Nevertheless, this variation was minor. Figures 1 and 2 highlight the contrasting visuals in relation to surfaces without and with chemical treatment. The real and apparent rice husk densities are higher than that for pine cone shell (Almeandros et al. 2015) and similar to those of the brown algae

Sargassum filipendula (Cardoso et al. 2018). On the other hand, Ferreira et al. (2018) presented higher values for coconut fibre.

FTIR

The activation procedure was able to modify the functional groups presented in the biomass (Table 2 and Fig. S1) and to change both types of biomass significantly.

For the rice husk (Fig. S1a), the activation was most significant at 550 cm⁻¹, indicating an absence of the silicic acid functional group. On the other hand, activated coffee husk recorded the absence of three functional groups: -CH, ether, and alkene (Fig. S1b).

Biosorption assays

Kinetics experiments

Figure 3 reports the results of biosorption as a function of time for U (total) (a), ²⁴¹Am (b), and ¹³⁷Cs (c) using coffee or rice husk, in raw and activated forms.

The kinetics results for removal of the three radioactive species showed that equilibrium was reached after 2 h for all biomass. Shehee et al. (2012) reported that the time to reach equilibrium for the removal of U and Pu by titanium-based materials was 96 h. Tripathi et al. (2011) found that 3 h was enough to achieve equilibrium for the sorption of ²⁴¹Am in the presence of other radionuclides. Interestingly, our results were superior in terms of time to reach equilibrium.

Table S2 details the biosorption capacity at equilibrium in kinetics experiments. The measured biosorption capacities were those obtained after the equilibrium time (2 h). The highest experimental sorption capacities were obtained with raw coffee husk for all radionuclides, followed by activated coffee husk for uranium sorption. For the sorption of americium and caesium, activated husks showed similar capability.

The absolute masses of ²⁴¹Am and ¹³⁷Cs removed were much lower than those for uranium, since their initial concentrations were much lower. Note that actual radioactive waste was utilised in this work; therefore, the addition of americium

and/or caesium would be inappropriate. It is important to emphasise that the affinity obtained was also influenced by the initial concentration of the radionuclides studied. The affinity behaviour may change drastically when working with initial concentrations with different orders of magnitude (Volesky 2003). This impeded a thorough affinity analysis between the elements and the biomass.

In the case of coffee husks, the activation process caused changes in the structure that slightly reduced the uranium sorption capacity (raw coffee husk 1.96 ± 0.04 mg g⁻¹ versus 1.76 ± 0.04 mg g⁻¹ for activated coffee husk). As for rice husk, the activation process resulted in an increased sorption capacity (raw rice husk 0.47 ± 0.13 mg g⁻¹ versus 0.82 ± 0.04 mg g⁻¹ for activated rice husk), probably due to the removal of ions which compete for the adsorption sites. According to Rocha et al. (2009), rice straw is composed of cellulose, hemicellulose, lignin, extractives, water, and mineral ash, presenting a large amount of SiO₂. By the activation process, lignin is immediately available to combine with cations by proton exchange and chelation with the metallic ions.

A prediction based on the ionic properties of the metals involved in a multi-metal system can assist in understanding the adsorption mechanism. The results indicate that U(VI) is the most adsorbed ion among the three metal ions studied, since it has better accessibility to the pores as it has the smallest ionic radius compared with Am and Cs (Table 3). Moreover, since hydrated radii increase as a function of atomic number in the actinide series (increased covalency increases the number of water ligands), Am also has a higher hydrated radius compared with U, indicating less accessibility of the Am ion (Katz et al. 1987). The highest standard reduction potential (Table 3) observed was for U, exhibiting a stronger ionic interaction with the electron-rich surface of the adsorbents (Mohan and Singh 2002).

Biosorption studies of ternary systems (e.g. uranium, americium, and caesium) are scarce in the literature. In fact, the only work found that studied the ternary system for these three chemical elements was that previously published by Ferreira et al. (2018). However, there are biosorption studies of single elements in simulated waste that can provide an indirect comparison.

Table 3 Ionic properties of uranium, americium, and caesium (Katz et al. 1987; Krestou et al. 2003)

Property	U(VI)	Am(III)	Cs(I)
Atomic weight	238.02891	243	132.90545
Electronic configuration	Rn 5f3 6d1 7s2	Rn 5f7 7s2	[Xe] 6s1
Electronegativity	1.38	1.3	0.79
Ionic radius (Å)	1.75	2.00	3.00
Coordination number	5	10.3	> 6
Standard reduction pot. (V)	U ³⁺ + 3e ⁻ ⇌ U(s) (-1.66) U ⁴⁺ + e ⁻ ⇌ U ³⁺ (-0.52)	Am ³⁺ + 3e ⁻ ⇌ Am(s) (-2.07)	Cs ⁺ (aq) + e ⁻ ⇌ Cs(s) (-2.92)

Table 4 Isotherm parameters measured for raw and activated rice husk

Parameters/models	Raw rice husk				Activated rice husk			
	Langmuir ternary adsorption model	Langmuir ternary with two sites	Jain and Snoeyink ternary model	Modified Jain and Snoeyink ternary model	Langmuir ternary adsorption model	Langmuir ternary with two sites	Jain and Snoeyink ternary model	Modified Jain and Snoeyink ternary model
$q_{\max 1}$ (mmol g ⁻¹)	3.29×10^{-6}	9.62×10^{-4}	2.87×10^{-6}	2.61×10^{-6}	5.79×10^{-6}	1.92×10^{-10}	6.15×10^{-6}	5.74×10^{-6}
b_1 (L mmol ⁻¹)	3.75×10^3	-	2.83×10^3	2.79×10^3	8.98×10^3	-	9.15×10^3	8.16×10^3
b_2 (L mmol ⁻¹)	8.75×10^3	13.8	9.61×10^3	1.09×10^4	1.97×10^4	3.63×10^8	1.85×10^4	1.85×10^4
b_3 (L mmol ⁻¹)	3.02×10^4	51.9	2.98×10^4	2.97×10^4	4.56×10^3	1.05×10^8	4.46×10^3	4.53×10^3
$q_{\max 2}$ (mmol g ⁻¹)	-	2.69×10^6	9.43×10^{-7}	1.21×10^{-6}	-	3.69×10^{-6}	2.62×10^{-17}	6.85×10^{-7}
bb_1 (L mmol ⁻¹)	-	5.61×10^3	-	2.92×10^3	-	4.10×10^4	-	1.71×10^4
ADD ₁	5.50	3.14	25.62	7.38	16.84	7.70	15.45	15.94
ADD ₂	31.04	41.91	32.73	32.81	11.96	12.75	11.85	11.49
ADD ₃	22.57	0.17	18.37	17.53	9.53	7.97	10.07	8.55
ADD (average)	19.70	15.07	25.57	19.24	12.78	9.47	12.46	11.99

Yi et al. (2016b) studied coconut husk activated carbon (CHAC) as a biosorbent for the uptake of U(VI) from aqueous solutions. They found that the maximum capacity of CHAC was 6.67 mg g^{-1} , which is superior to ours (max = 1.96 mg g^{-1}). Luo et al. (2003) evaluated *Candida* sp. for the biosorption of ^{241}Am in the presence and absence of Au^{3+} or Ag^+ . The values they obtained were far superior to ours, with a maximum capacity of $501.8 \times 10^{-3} \text{ mg g}^{-1}$. Mishra et al. (2007) studied the biosorption of caesium by rice husk. They studied the removal in terms of radioactive activity and observed a reduction of between 9 and 4200 Bq g^{-1} ($(1.77 \times 10^{-10}$ to $852.00 \times 10^{-10} \text{ mg g}^{-1})$, (1.32×10^{-13} to $636.00 \times 10^{-13} \text{ mmol g}^{-1}$)). The biosorption of ^{137}Cs observed in the present study is similar to that found by Mishra et al. (2007). According to these authors, the low sorption capacity of caesium can be justified by the high concentration of hydrogen ions in the medium (our work pH = 2.17). In the presence of caesium ions, competition between these elements can occur through the binding sites present in the rice husk, reducing their adsorption. Recently, Lee et al. (2019) employed microalgae to remove radioactive caesium from contaminated water. They observed a different result compared with our work, with 95% removal of soluble ^{137}Cs in 48 h using *Haematococcus pluvialis* red cyst, and both *H. pluvialis* intermediate cells and *Chlorella vulgaris* showed 90% uptake efficiency of ^{137}Cs despite the slow uptake rate.

Ferreira et al. (2018) demonstrated different sorption capacities using raw and activated coconut fibres. Concerning maximum sorption capacity, the present work highlighted greater uranium sorption (raw coffee husk $1.96 \pm 0.04 \text{ mg g}^{-1}$ versus raw coconut fibre $1.82 \pm 0.04 \text{ mg g}^{-1}$), lower americium sorption (raw coffee husk $39.4 \pm 1.8 \times 10^{-6} \text{ mg g}^{-1}$ versus activated coconut fibre $73.4 \pm 5.3 \times 10^{-6} \text{ mg g}^{-1}$), and similar caesium sorption (raw coffee husk $46.6 \pm 4.1 \times 10^{-9} \text{ mg g}^{-1}$ versus raw coconut fibre $44.7 \pm 8.9 \times 10^{-9} \text{ mg g}^{-1}$).

Sorption isotherms

Langmuir, two-site Langmuir, Jain and Snoeyink, and modified Jain and Snoeyink ternary systems were used to describe the experimental data in terms of mathematical expressions (Table 1). Tables 4 and 5 show the values obtained for the following parameters: $q_{\max 1}$ models (maximum biosorption capacity at site 1), b (adsorption and desorption rate), $q_{\max 2}$ (maximum biosorption capacity at site 2), bb_1 (adsorption rate and uranium desorption at the two sites), ADD_i (relative error, $i = (1)$ uranium, (2) americium, (3) caesium), and ADD average (average relative error of the three metals). Figures 4, 5, 6, and 7 depict the experimental and calculated values for raw and activated forms of coffee and rice husks.

According to the calculated ADD values, the biosorption process for the raw and activated rice husks was best

Table 5 Isotherm parameters measured for raw and activate coffee husk

Parameters/models	Raw coffee husk				Activated coffee husk			
	Langmuir ternary adsorption model	Langmuir ternary with two sites	Jain and Snoeyink ternary model	Modified Jain and Snoeyink ternary model	Langmuir ternary adsorption model	Langmuir ternary with two sites	Jain and Snoeyink ternary model	Modified Jain and Snoeyink ternary model
q_{max1} (mmol g ⁻¹)	1.24×10^{-5}	5.46×10^{-3}	1.48×10^{-5}	1.37×10^{-5}	8.20×10^{-6}	3.09×10^{-3}	7.71×10^{-6}	7.61×10^{-6}
b_1 (L mmol ⁻¹)	5.34×10^3	-	5.55×10^3	3.85×10^3	1.37×10^4	-	1.23×10^4	1.10×10^4
b_2 (L mmol ⁻¹)	7.16×10^3	7.83	5.84×10^3	5.49×10^3	1.13×10^4	7.74	1.14×10^4	1.07×10^4
b_3 (L mmol ⁻¹)	2.07×10^2	0.24	1.76×10^2	1.64×10^2	5.63×10^2	0.42	5.43×10^2	5.16×10^2
q_{max2} (mmol g ⁻¹)	-	9.20×10^{-6}	1.54×10^{-7}	2.86×10^{-6}	-	1.15×10^{-5}	7.48×10^{-7}	6.28×10^{-7}
bb_1 (L mmol ⁻¹)	-	2.38×10^4	-	8.42×10^4	-	5.86×10^3	-	1.27×10^4
ADD ₁	29.24	5.72	21.15	11.72	13.12	3.02	11.34	9.94
ADD ₂	3.25	21.14	2.54	4.32	21.68	40.23	22.18	23.05
ADD ₃	8.63	14.47	9.22	6.65	15.86	32.21	15.10	14.60
ADD (average)	13.71	13.78	10.97	7.57	16.88	25.15	16.20	15.86

represented by the Langmuir ternary isotherm model with two sites, indicating that the adsorption of uranium occurs at a site other than that for americium and caesium. ADD is the mean error of the value predicted by the model in relation to the experimental value. The smaller this error, the better the fit;

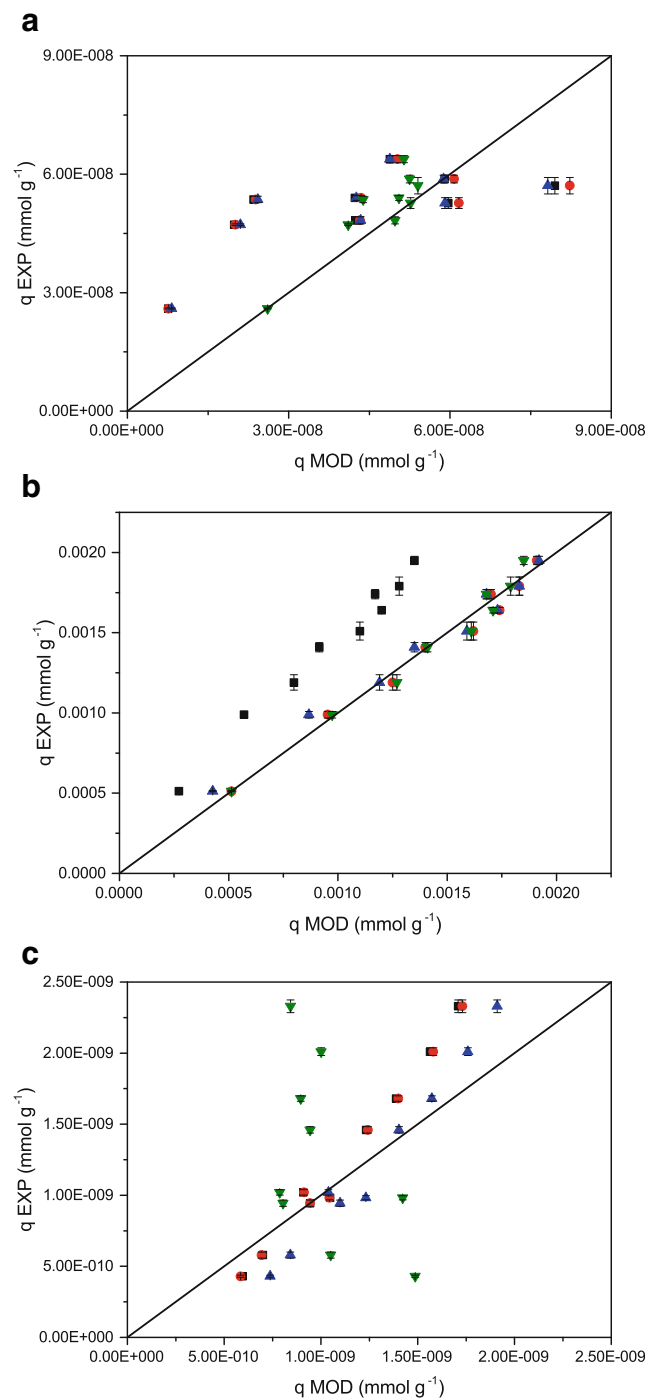


Fig. 4 Experimental adsorption equilibrium data for raw rice husk versus the models. **a** Uranium. **b** Americium. **c** Caesium. □, black Langmuir ternary adsorption. ○, red Langmuir ternary with two sites. ▲, blue Jain and Snoeyink ternary. ▼, green Modified Jain and Snoeyink ternary. ◆ Uranium. □ Americium. ▲ Caesium

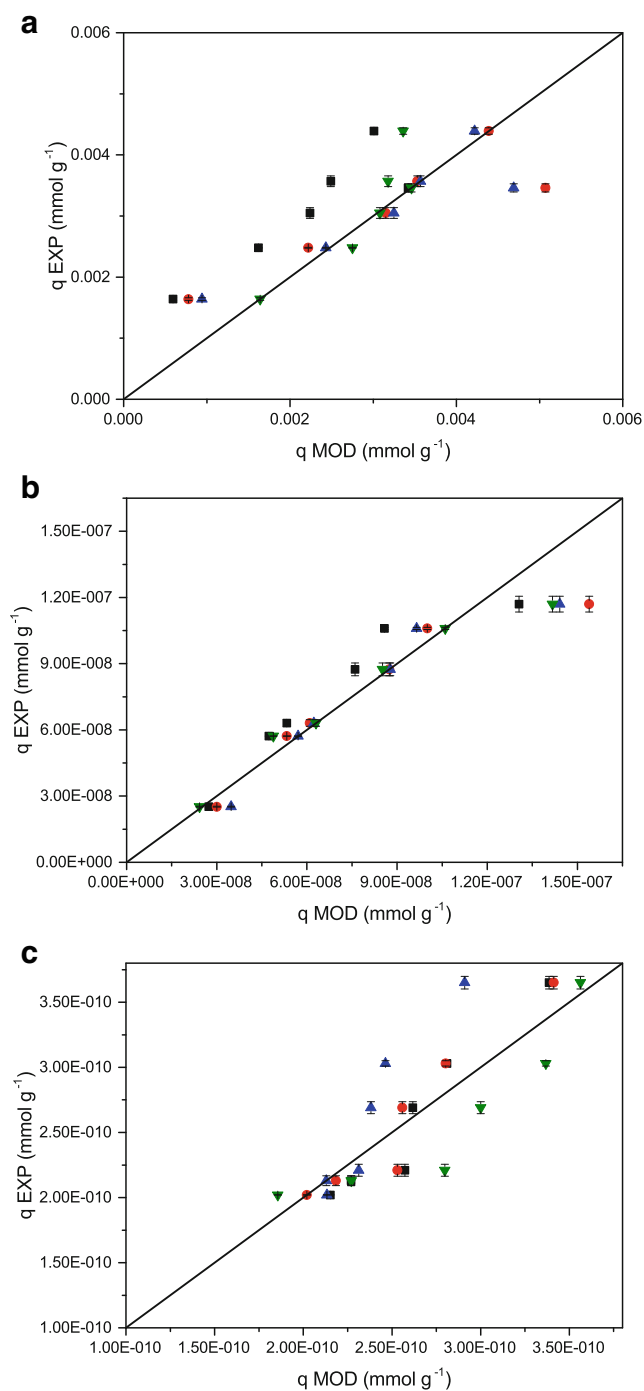


Fig. 5 Experimental adsorption equilibrium data for activated rice husk versus the models. **a** Uranium. **b** Americium. **c** Caesium. □, black Langmuir ternary adsorption. ○, red Langmuir ternary with two sites. ▲, blue Jain and Snoeyink ternary. ▼, green Modified Jain and Snoeyink ternary. ◆ Uranium. □ Americium. ▲ Caesium

consequently, this parameter can be used to choose the best model. For the coffee husk, in the raw and activated states, the biosorption process was best described by the modified Jain and Snoeyink ternary model that considers the presence of two types of site that have different adsorption energies. It is important to note that the estimated values of the parameter

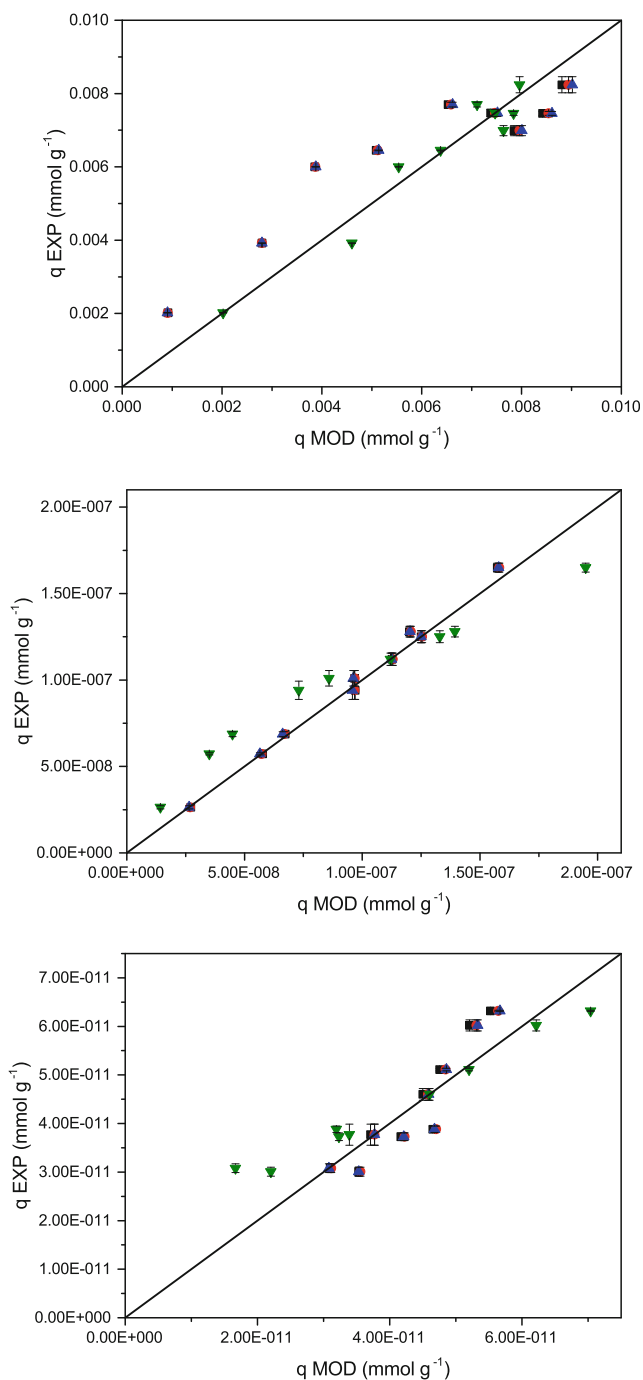


Fig. 6 Experimental adsorption equilibrium data for raw coffee husk versus the models. **a** Uranium. **b** Americium. **c** Caesium. □, black Langmuir ternary adsorption. ○, red Langmuir ternary with two sites. ▲, blue Jain and Snoeyink ternary. ▼, green Modified Jain and Snoeyink ternary. ◆ Uranium. □ Americium. ▲ Caesium

q_{max1} (uranium) are mostly in the same order of magnitude (10^{-6}) as the experimental values. The b parameter of the isotherms is related to the affinity of the metal for the sites of the adsorbent material. The values of these parameters when compared with the raw and activated biomasses were different. Therefore, the chemical treatment modified the

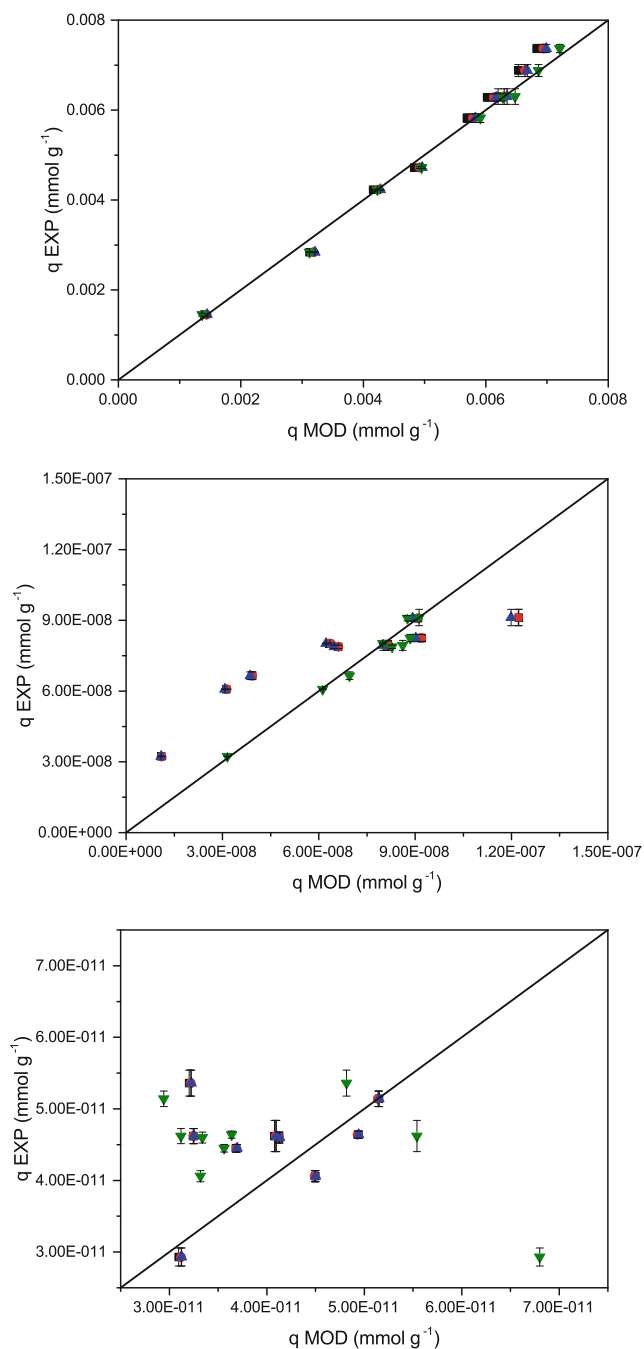


Fig. 7 Experimental adsorption equilibrium data for activated rice husk versus the models. **a** Uranium. **b** Americium. **c** Caesium. □, black Langmuir ternary adsorption. ○, red Langmuir ternary with two sites. ▲, blue Jain and Snoeyink ternary. ▼, green Modified Jain and Snoeyink ternary. ◆ Uranium. □ Americium. ▲ Caesium

properties of the adsorbent and, consequently, influenced the adsorption capacity. The affinity sequence given by parameter b varied depending on the biomass and its form: (raw rice husk) b_3 (^{137}Cs) $>$ b_2 (^{241}Am) $>$ b_1 (U), (activated rice husk) b_2 (^{241}Am) $>$ b_1 (U) $>$ b_3 (^{137}Cs) or b_3 (^{137}Cs) $>$ b_2 (^{241}Am) $>$ b_1 (U), (raw coffee husk) b_2 (^{241}Am) $>$ b_1 (U) $>$ b_3 (^{137}Cs), and (activated coffee husk) b_1 (U) $>$ b_2 (^{241}Am) $>$ b_3 (^{137}Cs).

Biosorption kinetics

The two-site Langmuir, and Jain and Snoeyink ternary models were selected from the results obtained from adjustment of the equilibrium data. These models were used to evaluate the kinetics of metal removal. Tables S3 and S4 show the parameter values obtained for these models, respectively. The full concentration profiles of experimental and modelling data are also shown in the supporting information (Figs. S2, S3, S4, and S5). The parameters evaluated are $q_{\text{max}1}$, k_i (adsorption rate), k_{-i} (desorption rate), Sa (binding site 1), Sb (binding site 2), $q_{\text{max}2}$, bb_1 , ADD_i (relative error), and ADD (average) (mean relative error for the three metals). Indices 1, 2, and 3 refer respectively to the metals: uranium (total), americium, and caesium.

Conclusions

The effect of rice and coffee husks (raw and chemically activated) on the adsorption of U (total), ^{241}Am , and ^{137}Cs in real liquid organic radioactive waste is presented and analysed in this work for the first time in literature. Another point of interest is the prediction based on the ionic properties of U, Am, and Cs, which explained the different sorption capacities observed. To the best of our knowledge, there is no report of such prediction for these three elements with experimental data validation. Activation by acid/base treatment resulted in increased sorption capacity for rice husk and decreased sorption capacity for coffee husk, and slightly modified surface area of both materials. The values of maximum adsorption capacity for raw rice husk were $0.47 \pm 0.13 \text{ mg g}^{-1}$ (U (total)), $14.4 \pm 0.5 \times 10^{-6} \text{ mg g}^{-1}$ (^{241}Am), and $19.8 \pm 1.4 \times 10^{-9} \text{ mg g}^{-1}$ (^{137}Cs). For activated rice husk, the values were $0.82 \pm 0.04 \text{ mg g}^{-1}$ (U (total)), $27.2 \pm 1.5 \times 10^{-6} \text{ mg g}^{-1}$ (^{241}Am), and $45.2 \pm 8.9 \times 10^{-9} \text{ mg g}^{-1}$ (^{137}Cs). For raw coffee husk, the values were $1.96 \pm 0.04 \text{ mg g}^{-1}$ (U (total)), $39.4 \pm 1.8 \times 10^{-6} \text{ mg g}^{-1}$ (^{241}Am), and $46.6 \pm 4.1 \times 10^{-9} \text{ mg g}^{-1}$ (^{137}Cs). For activated coffee husk, the values were $1.76 \pm 0.04 \text{ mg g}^{-1}$ (U (total)), $25.9 \pm 3.6 \times 10^{-6} \text{ mg g}^{-1}$ (^{241}Am), and $43.8 \pm 4.0 \times 10^{-9} \text{ mg g}^{-1}$ (^{137}Cs). In the kinetics tests, equilibrium was reached after 2 h of contact for all biomass and elements. The ternary isotherm and kinetics models were effective for evaluating the simultaneous biosorption of uranium, caesium, and americium in LORW. All biosorbents demonstrated biosorption capacity. However, the raw coffee husk was the most suitable for the treatment of liquid waste containing U (total), ^{241}Am , and ^{137}Cs , because of its higher sorption capacity in comparison with the rice husk. Low sorption capacity for ^{137}Cs was identified and explained by the low pH (2.17) of the waste studied because of the high concentration of hydrogen ions in the medium, which competed for the biomass binding sites. Further work is required to identify

the major functional groups involved in metal recovery by these types of biomass. A thorough analysis of these compounds is also necessary for a more in-depth discussion of why each type of biomass produced different results when used to adsorb these radionuclides. Finally, the determination of the thermodynamic parameters is also needed for a better understanding of the process.

Acknowledgements We are thankful to Dr. Flavia R.O. Silva and the Laboratório de Microscopia e Microanálise (LMM/IPEN) for the SEM/EDS analyses.

Funding information This research was supported by the Nuclear and Energy Research Institute, the Brazilian National Nuclear Energy Commission, and the Brazilian National Council for Scientific and Technological Development.

References

- Ajmal M, Ali Khan Rao R, Anwar S, Ahmad J, Ahmad R (2003) Adsorption studies on rice husk: removal and recovery of Cd(II) from wastewater. *Bioresour Technol* 86:147–149. [https://doi.org/10.1016/S0960-8524\(02\)00159-1](https://doi.org/10.1016/S0960-8524(02)00159-1)
- Alhogbi BG (2017) Potential of coffee husk biomass waste for the adsorption of Pb(II) ion from aqueous solutions. *Sustain Chem Pharm* 6:21–25. <https://doi.org/10.1016/j.scp.2017.06.004>
- Almeandros AI, Martín-Lara MA, Ronda A, Pérez A, Blázquez G, Calero M (2015) Physico-chemical characterization of pine cone shell and its use as biosorbent and fuel. *Bioresour Technol* 196:406–412. <https://doi.org/10.1016/j.biortech.2015.07.109>
- Bağda E, Tuzen M, Sari A (2017) Equilibrium, thermodynamic and kinetic investigations for biosorption of uranium with green algae (*Cladophora hutchinsiae*). *J Environ Radioact* 175–176:7–14. <https://doi.org/10.1016/j.jenvrad.2017.04.004>
- Bai J, Yao H, Fan F, Lin M, Zhang L, Ding H, Lei F, Wu X, Li X, Guo J, Qin Z (2010) Biosorption of uranium by chemically modified *Rhodotorula glutinis*. *J Environ Radioact* 101:969–973. <https://doi.org/10.1016/J.JENVRAD.2010.07.003>
- Cardoso SL, Costa CSD, da Silva MGC, Vieira MGA (2018) Dealginated seaweed waste for Zn(II) continuous removal from aqueous solution on fixed-bed column. *J Chem Technol Biotechnol* 93:1183–1189. <https://doi.org/10.1002/jctb.5479>
- Chakraborty D, Maji S, Bandyopadhyay A, Basu S (2007) Biosorption of cesium-137 and strontium-90 by mucilaginous seeds of *Ocimum basilicum*. *Bioresour Technol* 98:2949–2952. <https://doi.org/10.1016/j.biortech.2006.09.035>
- Dhami PS, Kannan R, Naik PW, et al (2002) Biosorption of americium using biomasses of various *Rhizopus* species. 885–889
- Febrianto J, Kosasih AN, Sunarso J, Ju YH, Indraswati N, Ismadji S (2009) Equilibrium and kinetic studies in adsorption of heavy metals using biosorbent: a summary of recent studies. *J Hazard Mater* 162: 616–645. <https://doi.org/10.1016/j.jhazmat.2008.06.042>
- Ferreira RVP, Dutra F, Bellini MH et al (2012) Treatment of radioactive liquid organic waste using bacteria community. *J Radioanal Nucl Chem* 291:811–817. <https://doi.org/10.1007/s10967-011-1564-2>
- Ferreira RVP, Silva EA, Canevesi RLS, Ferreira EGA, Taddei MHT, Palmieri MC, Silva FRO, Marumo JT (2018) Application of the coconut fiber in radioactive liquid waste treatment. *Int J Environ Sci Technol* 15:1629–1640. <https://doi.org/10.1007/s13762-017-1541-6>
- Katz J, Seaborg GT, Morss LR (1987) The chemistry of the actinide elements. Springer Netherlands, Dordrecht
- Korotkova TG, Ksandopulo SJ, Donenko AP, et al (2016) Physical properties and chemical composition of the rice husk and dust. *Orient J Chem* 32:3213–3219. <https://doi.org/10.13005/ojc/320644>
- Krestou A, Xenidis A, Papias D (2003) Mechanism of aqueous uranium (VI) uptake by natural zeolitic tuff. *Miner Eng* 16:1363–1370. <https://doi.org/10.1016/j.mineng.2003.08.012>
- Krishnani KK, Meng X, Boddu VM (2008) Fixation of heavy metals onto lignocellulosic sorbent prepared from paddy straw. *Water Environ Res* 80:2165–2174. <https://doi.org/10.2175/106143008X304785>
- Kumar U, Bandyopadhyay M (2006) Sorption of cadmium from aqueous solution using pretreated rice husk. *Bioresour Technol* 97:104–109. <https://doi.org/10.1016/j.biortech.2005.02.027>
- Lee K-Y, Lee S-H, Lee JE, Lee S-Y (2019) Biosorption of radioactive cesium from contaminated water by microalgae *Haematococcus pluvialis* and *Chlorella vulgaris*. *J Environ Manag* 233:83–88. <https://doi.org/10.1016/j.jenvman.2018.12.022>
- Li Y, Liu F, Xia B, du Q, Zhang P, Wang D, Wang Z, Xia Y (2010) Removal of copper from aqueous solution by carbon nanotube/calcium alginate composites. *J Hazard Mater* 177:876–880. <https://doi.org/10.1016/j.jhazmat.2009.12.114>
- Liao J, Yang Y, Luo S, Liu N, Jin J, Zhang T, Zhao P (2004) Biosorption of americium-241 by immobilized *Rhizopus arrhizus*. *Appl Radiat Isot* 60:1–5. <https://doi.org/10.1016/J.APRADISO.2003.10.001>
- Liu N, Luo S, Yang Y, Zhang T, Jin J, Liao J (2002) Biosorption of americium-241 by *Saccharomyces cerevisiae*. *J Radioanal Nucl Chem* 252:187–191. <https://doi.org/10.1023/A:1015276813386>
- Lu X, Zhou X-j, Wang T-s (2013) Mechanism of uranium(VI) uptake by *Saccharomyces cerevisiae* under environmentally relevant conditions: batch, HRTEM, and FTIR studies. *J Hazard Mater* 262:297–303. <https://doi.org/10.1016/j.jhazmat.2013.08.051>
- Luo BS, Liu N, Yang Y, et al (2003) Biosorption of americium-241 by *Candida* sp. 318:315–318
- Ma Y, Lin J, Zhang C, Ren Y, Lin J (2011) Cd(II) and As(III) bioaccumulation by recombinant *Escherichia coli* expressing oligomeric human metallothioneins. *J Hazard Mater* 185:1605–1608. <https://doi.org/10.1016/j.jhazmat.2010.10.051>
- Mishra SP, Prasad SK, Dubey RS, Mishra M, Tiwari D, Lee SM (2007) Biosorptive behaviour of rice hulls for Cs-134 from aqueous solutions: a radiotracer study. *Appl Radiat Isot* 65:280–286. <https://doi.org/10.1016/j.apradiso.2006.09.007>
- Mohan D, Singh KP (2002) Single- and multi-component adsorption of cadmium and zinc using activated carbon derived from bagasse-an agricultural waste. *Water Res* 36:2304–2318. [https://doi.org/10.1016/S0043-1354\(01\)00447-X](https://doi.org/10.1016/S0043-1354(01)00447-X)
- Oliveira LS, Franca AS, Alves TM, Rocha SDF (2008a) Evaluation of untreated coffee husks as potential biosorbents for treatment of dye contaminated waters. *J Hazard Mater* 155:507–512. <https://doi.org/10.1016/j.jhazmat.2007.11.093>
- Oliveira WE, Franca AS, Oliveira LS, Rocha SD (2008b) Untreated coffee husks as biosorbents for the removal of heavy metals from aqueous solutions. *J Hazard Mater* 152:1073–1081. <https://doi.org/10.1016/j.jhazmat.2007.07.085>
- Pang C, Liu Y-H, Cao X-H, Li M, Huang GL, Hua R, Wang CX, Liu YT, An XF (2011) Biosorption of uranium(VI) from aqueous solution by dead fungal biomass of *Penicillium citrinum*. *Chem Eng J* 170:1–6. <https://doi.org/10.1016/J.CEJ.2010.10.068>
- Raoul TTD, Gabche AS, Mbadam KJ et al (2014) Kinetics and equilibrium studies of adsorption of phenol in aqueous solution onto activated carbon prepared from rice and coffee husks. *Int J Eng Tech Res* 2:166–173
- Rocha CG, Zaia DAM, da Silva Alfaya RV, da Silva Alfaya AA (2009) Use of rice straw as biosorbent for removal of Cu(II), Zn(II), Cd(II)

- and Hg(II) ions in industrial effluents. *J Hazard Mater* 166:383–388. <https://doi.org/10.1016/j.jhazmat.2008.11.074>
- Saini AS, Melo JS (2015) Biosorption of uranium by human black hair. *J Environ Radioact* 142:29–35. <https://doi.org/10.1016/J.JENVRAD.2015.01.006>
- Shehee TC, Elvington MC, Rudisill TS, Hobbs DT (2012) Separation of actinides and fission products using titanium-based materials. *Solvent Extr Ion Exch* 30:669–682. <https://doi.org/10.1080/07366299.2011.639262>
- Ting YP, Lawson F, Prince IG (1991) Uptake of cadmium and zinc by the alga *Chlorella vulgaris*: II. Multi-ion situation *BiotechnolBioeng* 37:445–455
- Tripathi SC, Kannan R, Dhami PS, Naik PW, Munshi SK, Dey PK, Salvi NA, Chattopadhyay S (2011) Modified *Rhizopus arrhizus* biomass for sorption of ²⁴¹Am and other radionuclides. *J Radioanal Nucl Chem* 287:691–695. <https://doi.org/10.1007/s10967-010-0949-y>
- Vieira LC, de Araujo LG, Ferreira RVP et al (2019) Uranium biosorption by *Lemma* sp. and *Pistia stratiotes*. *J Environ Radioact* 203:179–186. <https://doi.org/10.1016/j.jenvrad.2019.03.019>
- Volesky B (2003) Biosorption process simulation tools. *Hydrometallurgy* 71:179–190. [https://doi.org/10.1016/S0304-386X\(03\)00155-5](https://doi.org/10.1016/S0304-386X(03)00155-5)
- Wan Ngah WS, Hanafiah MAKM (2008) Removal of heavy metal ions from wastewater by chemically modified plant wastes as adsorbents: a review. *Bioresour Technol* 99:3935–3948. <https://doi.org/10.1016/j.biortech.2007.06.011>
- Wang J-s, Hu X-j, Wang J et al (2010) The tolerance of *Rhizopus arrhizus* to U(VI) and biosorption behavior of U(VI) onto *R. arrhizus*. *Biochem Eng J* 51:19–23. <https://doi.org/10.1016/j.bej.2010.04.010>
- Wang F, Tan L, Liu Q, Li R, Li Z, Zhang H, Hu S, Liu L, Wang J (2015) Biosorption characteristics of uranium (VI) from aqueous solution by pollen pini. *J Environ Radioact* 150:93–98. <https://doi.org/10.1016/J.JENVRAD.2015.07.002>
- Wang Y, Nie X, Cheng W et al (2019) A synergistic biosorption and biomineralization strategy for *Kocuria* sp. to immobilizing U(VI) from aqueous solution. *J Mol Liq* 275:215–220. <https://doi.org/10.1016/J.MOLLIQ.2018.11.079>
- Wei Y, Chen Z, Song H, et al (2019) The immobilization mechanism of U(VI) induced by *Bacillus thuringiensis* 016 and the effects of coexisting ions. *Biochem Eng J* 144:57–63. S1369703X19300130
- Yi Z-j, Yao J, Chen H-l et al (2016a) Uranium biosorption from aqueous solution onto *Eichhornia crassipes*. *J Environ Radioact* 154:43–51. <https://doi.org/10.1016/j.jenvrad.2016.01.012>
- Yi Z, Yao J, Kuang Y, Chen HL, Wang F, Xu JS (2016b) Uptake of hexavalent uranium from aqueous solutions using coconut husk activated carbon. *Desalin Water Treat* 3994:1–7. <https://doi.org/10.1080/19443994.2014.977956>
- Zheng XY, Shen YH, Wang XY, Wang TS (2018) Effect of pH on uranium(VI) biosorption and biomineralization by *Saccharomyces cerevisiae*. *Chemosphere* 203:109–116. <https://doi.org/10.1016/J.CHEMOSPHERE.2018.03.165>

Publisher's note Springer Nature remains neutral with regard to jurisdictional claims in published maps and institutional affiliations.